



Optically pumped flexible GaN-based ultraviolet VCSELs

YANG MEI,^{1,2}  PENG GU,¹ SHUAI YANG,¹ LEIYING YING,¹ AND BAOPING ZHANG^{1,2,*}

¹Laboratory of Micro/Nano-Optoelectronics, Department of Microelectronics and Integrated Circuits, Xiamen University, Xiamen 361005, China

²College of Photonics and Electronics, Minnan Science and Technology University, Quanzhou 362332, China

*bzhang@xmu.edu.cn

Received 8 January 2024; revised 19 February 2024; accepted 1 March 2024; posted 4 March 2024; published 28 March 2024

Flexible optoelectronic platforms, which integrate optoelectronic devices on a flexible substrate, are promising in more complex working environments benefiting from the mechanical flexibility. Herein, for the first time to the best of our knowledge, a flexible GaN-based vertical cavity surface-emitting laser (VCSEL) in the ultraviolet A (UVA) range was demonstrated by using a thin-film transfer process based on laser lift-off (LLO) and spin-coating of a flexible substrate. The lasing wavelength is 376.5 nm with a linewidth of 0.6 nm and threshold energy of 98.4 nJ/pulse, corresponding to a threshold energy density of 13.9 mJ/cm². The flexible substrate in this study is directly formed by spin-coating of photosensitive epoxy resin, which is much simplified and cost-effective, and a 2-in. wafer scale GaN-based membrane can be successfully transferred to a flexible substrate through this method. Such flexible UVA VCSELs are promising for the development of next-generation flexible and wearable technologies. © 2024 Optica Publishing Group

<https://doi.org/10.1364/OL.517756>

Flexible optoelectronic platforms which integrate high-performance electronic/photonics elements on a mechanically stretchable substrate have been attracting substantial attention and enable new applications in fields such as artificial photonic skin, diagnosis of diseases, deformable displays, and mechanical sensing [1–10]. Among them, flexible microcavity lasers are essential components not only for smart light sources but also for sensing applications. Benefiting from the deformable and stretchable characteristics, organic opto-materials and two-dimensional (2D) materials have been used to fabricate flexible microcavity lasers. Toward this end, different types of flexible microcavity lasers based on various organic and 2D materials have been successfully realized including Perovskite-based flexible VCSELs [3], dye doped PMMA-based flexible VCSELs/WGM lasers/micro fiber lasers [7,8], organic semiconducting polymer-based distributed feedback (DFB) membrane lasers [4], and 2D flexible random lasers generated by graphene oxide, single-layer graphene, hexagonal boron nitride, etc. [1]. However, organic or 2D light emitting materials are limited by the low efficiency, short lifespan, narrow photoconversion range, high temperature sensitivity, and complicated device fabrication processes. GaN-based semiconductors, on the other hand,

offer superior optical performance and reliability compared to organic optoelectronic materials, making them well-suited for a wide range of commercialized applications in areas such as solid-state lighting, display, and optical communications [11]. By modulating the alloy content, emission of GaN-based materials can cover a wide spectral range from deep ultraviolet to near infrared [12]. However, GaN-based materials face challenges in fabrication of flexible devices. One of the primary drawbacks of GaN is its inherent brittleness. The rigid nature of GaN makes it susceptible to cracking or fracturing when subjected to mechanical stress or bending. In addition, due to the limitation of single crystal material growth, the epitaxial layers of GaN-based materials usually need to be grown on a highly stable rigid substrate such as Si, sapphire, SiC, and GaN, under high temperature (>1000°C) [13]. This limitation poses challenges in the fabrication of GaN-based flexible optoelectronic devices. Nevertheless, GaN-based flexible optoelectronic devices including LEDs [14,15], micro-LEDs [16], strain gauges [6], piezoelectric sensors, and photodetectors [17] have been successfully reported by various groups through techniques such as substrate removal and thin-film transfer, forming nanostructures on a flexible substrate by low-temperature molecular beam epitaxy (MBE) [18], or growing GaN-based film on a flexible substrate through van der Waals epitaxy [19].

As for GaN-based flexible microcavity lasers, the reports are still rare because of the higher difficulty, and there are only few successful demonstrations. In 2019, Li *et al.* fabricated flexible GaN-based microdisk lasers on a PDMS substrate by using the laser lift-off (LLO) process to remove the sapphire substrate [20]. In 2021, Hu *et al.* fabricated a GaN-based microtubular cavity by electrochemical etching and then encapsulated the microtubule with a flexible PDMS substrate [10]. Recently in 2023, we also demonstrated ultraviolet microdisk lasers on a flexible PET substrate with a bottom dielectric distributed Bragg reflector (DBR) [2]. For GaN-based VCSELs which are featured with low threshold, circular beam profile, stable lasing wavelength, and fast modulation speed [21], however, there is still no report about their flexible counterparts.

In this study, for the first time to the best of our knowledge, flexible GaN-based VCSELs in the ultraviolet A (UVA) range were successfully fabricated by a simple and cost-effective fabrication process. The flexible substrate was formed by directly spin-coating photosensitive epoxy resin on the wafer surface,

which is more convenient and cost-effective when compared with other flexible lasers [10,20], and the original sapphire substrate was released by LLO. Through this method, a 2-in. wafer scale GaN-based thin film was successfully transferred to a very thin flexible substrate with thickness of $\sim 90\ \mu\text{m}$. The flexible VCSELs are featured with a double dielectric DBR structure, and optically pumped lasing at 376.5 nm in the UVA band was realized with an excitation threshold of 98.4 nJ/pulse. Such flexible UVA VCSELs are promising for the development of next-generation flexible and wearable optoelectronic technologies.

The epitaxial wafer used in this study was grown on (0001)-oriented sapphire substrate by using a metal-organic chemical vapor deposition (MOCVD) system. A low-temperature buffer layer was grown followed by a $2\ \mu\text{m}$ thick unintentionally doped GaN and a $2\ \mu\text{m}$ thick n-GaN. Then the active region containing five pairs of $\text{In}_{0.1}\text{Ga}_{0.9}\text{N}$ (3 nm)/GaN (5 nm) quantum wells (QWs) were grown. After that, a 20 nm thick p-AlGaIn electron blocking layer (EBL), a 97 nm thick p-GaN layer, and a 3 nm thick p+InGaIn layer were grown. The epi-layers are doped here, and they can also be used to fabricate electrically injected devices in the future. For the fabrication of UV VCSELs, different bonding and thin-film transfer techniques have been developed, including metal bonding together with electrochemical etching [22,23] and adhesive bonding together with LLO to remove the original substrate [24,25]. Lasing wavelengths of the UV VCSELs have extended from UVA to UVC. The latter method was chosen in this study to fabricate the flexible VCSELs. A dielectric DBR containing 12.5 pairs of $\text{TiO}_2/\text{SiO}_2$ was first deposited on the epitaxial wafer. Then, the sample was flip-chip bonded onto a temporary Si substrate by using photosensitive epoxy resin through spin-coating and UV curing. Subsequently, the original sapphire substrate was peeled off through LLO by using a pulsed 248-nm KrF excimer laser, similar with previous literature [26]. The temporary Si substrate here is to support the GaN membrane during the LLO process. The LLO process is also optimized in this study to obtain a flat surface after the removal of the sapphire substrate, and the root mean square roughness (RMS) of the surface after LLO is $\sim 0.9\ \text{nm}$ on a $5 \times 5\ \mu\text{m}^2$ area. The photoluminescence (PL) intensity of the active region did not show clear degradation after the LLO. Then the top dielectric DBR including seven pairs of $\text{TiO}_2/\text{SiO}_2$ was deposited to complete the UVA VCSEL structure. At last, the temporary Si substrate was removed, and the spin-coated photosensitive epoxy resin bonding material can directly act as the flexible substrate for the devices. The fabrication process of the flexible are shown in Fig. 1. The semiconductor membranes show no crack during the removal of the Si substrate, but the following flexible measurement will slightly break the device. This can be solved by etching the GaN-based membrane into separate tiny mesas after transferring to the flexible substrate [2].

The fabrication process here is much simplified when compared with traditional GaN-based flexible devices, and the thickness of the flexible substrate can be easily controlled by the spin-coating process, which is very thin of $\sim 90\ \mu\text{m}$ in this case. Through this method, a 2-in. wafer scale GaN-based membrane with bottom DBR was successfully transferred to the flexible substrate, as shown in Fig. 2(a). The amethyst color of the GaN-based membrane on the flexible substrate was caused by the color filtering of the bottom DBR. The photo of the fabricated flexible VCSELs with full structure was given in Fig. 2(b), showing good flexibility and transparency.

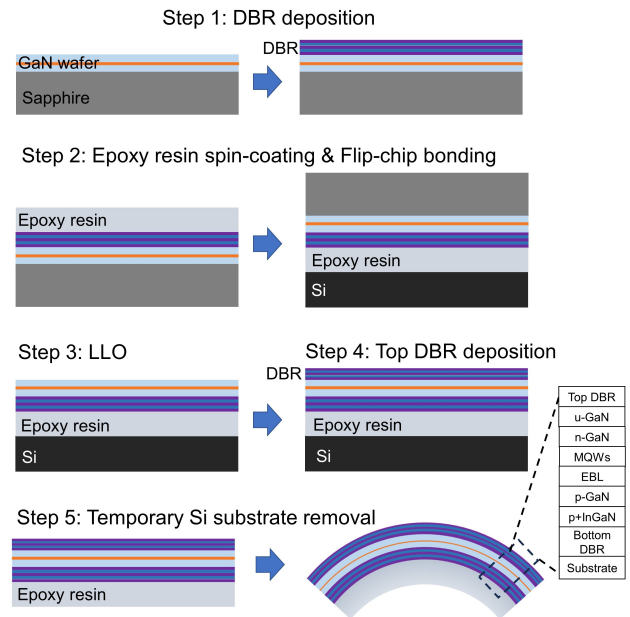


Fig. 1. Fabrication processes of the flexible VCSELs.

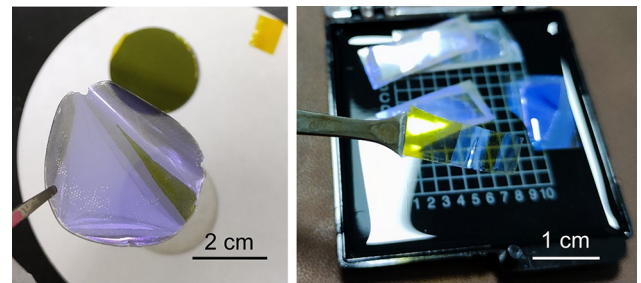


Fig. 2. (a) 2-inch GaN membrane transferred to flexible substrate. (b) As fabricated flexible VCSELs.

The PL spectra of the epitaxial wafer as well as the fabricated flexible VCSELs were measured by a micro-PL system at room temperature under excitation by a CryLas FTSS-355 Q1 355-nm pulsed laser with a repetition frequency of 15 kHz and a pulse width of 1 ns. The top dielectric DBR of the VCSEL in this study shows a transmittance window at around 355 nm, so that the 355 nm excitation laser was chosen here. The circular excitation laser spot was focused on the wafer surface with a diameter of $30\ \mu\text{m}$ by an objective lens (NA0.47, 40 \times). The output light of the sample was collected by the same objective lens and guided to the spectrometer for measurement. The PL spectrum of the as-grown QW wafer shows a spontaneous emission peak at around 420 nm under low excitation energy, as shown in Fig. 3. With increasing excitation energy, a new peak of 388 nm appeared at the high energy shoulder, and the linewidth of the spontaneous spectrum exhibited a sudden decrease to 3.2 nm, demonstrating the stimulated emission in the UVA band at room temperature. This demonstrates the high material gain and the potential to develop UVA VCSELs using the InGaIn active region with low Indium content.

After the fabrication of the full VCSEL structure, the sample was optically excited to study the lasing characteristics. Figure 4(a) shows the emission spectra at different excitation levels

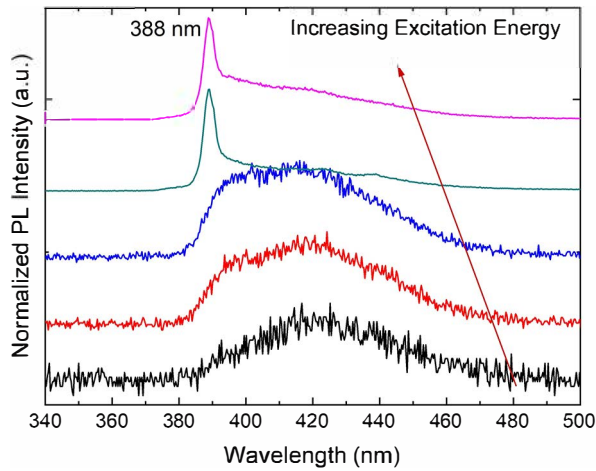


Fig. 3. PL spectra of the epi-wafer under different excitation levels.

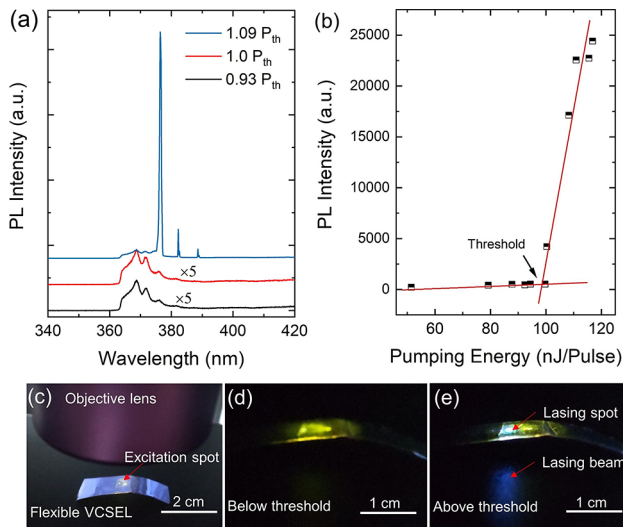


Fig. 4. (a) Lasing spectra of the flexible VCSEL under different excitation levels. (b) Output versus pumping energy of the flexible VCSELs. (c) Measurement system, and flexible VCSELs working (d) below threshold and (e) above threshold.

measured from the flexible VCSEL. The spectra with low excitation levels are enlarged for clarity, and several weak peaks attributed to the spontaneous emission of the cavity modes can be observed. The spectra of the spontaneous emission are asymmetric because there is a filter in our measurement system, and the emission with wavelength shorter than 363 nm was cut. The mode spacing $\Delta\lambda$ (free spectral range, FSR) was ~ 5 nm, and the effective cavity length L can be calculated to be ~ 4140 nm by the formula [2]:

$$L = \lambda^2 / (n_g \cdot \Delta\lambda), \quad (1)$$

where λ and n_g (~ 3.3 at 370 nm) are the mode wavelength and the group index of the cavity, respectively. The calculated cavity length consists well with the epi-thickness of the GaN wafer. With increasing excitation energy, a narrow peak emerges at 376.5 nm in the UVA band and increases significantly when the excitation energy exceeds the threshold. The linewidth of the cavity mode shows a sharp decrease from 2.8 to 0.6 nm, demonstrating the lasing action. Figure 4(b) shows the output intensity

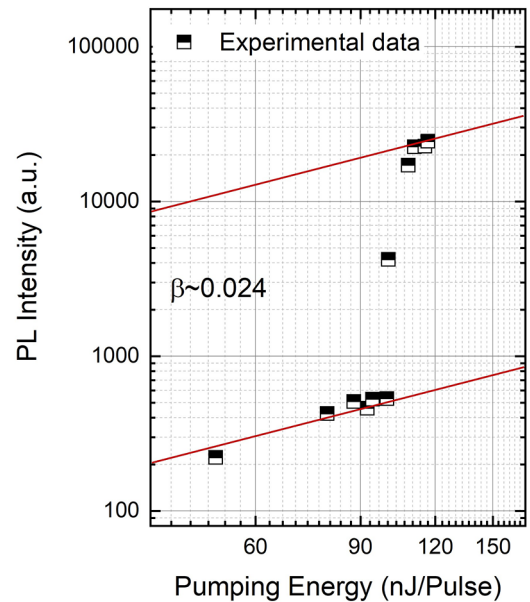


Fig. 5. Output intensity as a function of the excitation energy plotted in double logarithm coordinates.

as a function of excitation energy. The threshold energy was fitted as 98.4 nJ/pulse, corresponding to a threshold energy density of 13.9 mJ/cm². Figures 4(c)–(e) show the photographs of the measurement system and flexible VCSELs operating below and above the lasing threshold. The flexible device shows a yellow-emission color below threshold, which is caused by the excitation of the yellow-emission band of n-GaN and the low reflectivity of top DBR in the yellow band. When the excitation energy was increased beyond threshold, a bright lasing spot appeared, and the lasing beam can be clearly observed, proving unambiguously the lasing action. The output intensity as a function of the excitation energy plotted in double logarithm coordinates is shown in Fig. 5. The typical “S” shape of the output behavior demonstrates the lasing action, and the spontaneous coupling factor (β) is fitted to be ~ 0.024 . Electrically injected GaN-based flexible VCSELs were not realized in this study, and there are still difficulties at present. The design of electrically injected structure including electrode and intra-cavity contacting layers is very different in flexible VCSELs when compared with devices on the rigid substrate. The heat accumulation is also more serious in devices with an organic flexible substrate. Further work on fabricating electrically injected GaN-based flexible VCSELs is ongoing.

For the flexible devices, it is important to study the device performance under different strain states or bending condition. In our previous work, we fabricated flexible GaN-based microdisk lasers with a diameter of 20 μm on a PET substrate, and the lasing wavelength can be modulated by the external strain under different bending conditions [2]. This modulation effect is caused by the shift of the gain spectrum of the InGaN QW active region under different external strains. Similar measurement was also conducted with the flexible VCSELs in this study, however, without observing such phenomenon. The lasing wavelength of the flexible VCSEL is stable under different bending conditions. For the VCSEL with a short cavity in this study, the lasing wavelength of the cavity modes is mainly determined by the cavity length, which is less sensitive to the external strain.

In summary, optically pumped flexible GaN-based UVA VCSELs were fabricated for the first time. The VCSEL structure was transferred onto a flexible and transparent substrate formed by directly spin-coating a photosensitive epoxy resin layer, and wafer scale thin-film transfer has been demonstrated. The lasing wavelength of the device is 376.5 nm with a threshold energy of 98.4 nJ/pulse at room temperature. This study is promising for the development of GaN-based UV laser sources for wearable optoelectronics, flexible medical applications, and compact disinfection systems. In the future, by improving the device heat management and properly designing the electrode structure, flexible GaN-based VCSELs under electrical injection can be expected, broadening the possible applications of flexible GaN-based laser sources.

Funding. National Natural Science Foundation of China (62104204, 62174140, 62234011, U21A20493); Natural Science Foundation of Fujian Province (2023J05020); President's Foundation of Xiamen University (ZK1044).

Acknowledgment. The authors thank Lilong Ma for providing theoretical support.

Disclosures. The authors declare no conflicts of interest.

Data availability. Data underlying the results presented in this paper are not publicly available at this time but may be obtained from the authors upon reasonable request.

REFERENCES

1. H. W. Hu, G. Haider, Y. M. Liao, *et al.*, *Adv. Mater.* **29**, 1703549 (2017).
2. P. Gu, S. Yang, L. Ma, *et al.*, *Opt. Lett.* **48**, 4117 (2023).
3. S. Chen and A. Nurmikko, *ACS Photonics* **4**, 2486 (2017).
4. M. Karl, J. M. Glackin, M. Schubert, *et al.*, *Nat. Commun.* **9**, 1525 (2018).
5. T. Zhou, J. Zhou, Y. Cui, *et al.*, *Opt. Express* **26**, 16797 (2018).
6. Y. Peng, J. Lu, D. Peng, *et al.*, *Adv. Funct. Mater.* **29**, 1905051 (2019).
7. T. Ali, J. D. Lin, B. Snow, *et al.*, *Adv. Opt. Mater.* **8**, 1901891 (2020).
8. R. Chen, V. D. Ta, and H. Sun, *ACS Photonics* **1**, 11 (2014).
9. C. Zhang, H. Dong, C. Zhang, *et al.*, *Sci. Adv.* **7**, eabh3530 (2021).
10. P. Hu, Y. Li, S. Zhang, *et al.*, *Crystals* **11**, 1251 (2021).
11. S. Pimputkar, J. S. Speck, S. P. DenBaars, *et al.*, *Nat. Photonics* **3**, 180 (2009).
12. W. Sha, Q. Hua, J. Wang, *et al.*, *ACS Appl. Mater. Interfaces* **14**, 3000 (2022).
13. X. Chen, J. Dong, C. He, *et al.*, *Nano-Micro Lett.* **13**, 1 (2021).
14. M. Asad, Q. Li, M. Sachdev, *et al.*, *Nano Energy* **73**, 104724 (2020).
15. H. E. Lee, J. Choi, S. H. Lee, *et al.*, *Adv. Mater.* **30**, 1800649 (2018).
16. C. Goßler, C. Bierbrauer, R. Moser, *et al.*, *J. Phys. D: Appl. Phys.* **47**, 205401 (2014).
17. M. Peng, Y. Liu, A. Yu, *et al.*, *ACS Nano* **10**, 1572 (2016).
18. C. Zhao, T. K. Ng, R. T. Elafandy, *et al.*, *Nano Lett.* **16**, 4616 (2016).
19. F. Ren, B. Liu, Z. Chen, *et al.*, *Sci. Adv.* **7**, eabf5011 (2021).
20. K. H. Li, Y. F. Cheung, and H. W. Choi, *ACS Appl. Electron. Mater.* **1**, 1112 (2019).
21. Y. Mei, G.-E. Weng, B.-P. Zhang, *et al.*, *Light: Sci. Appl.* **6**, e16199 (2016).
22. F. Hjort, J. Enslin, M. Cobet, *et al.*, *ACS Photonics* **8**, 135 (2021).
23. G. Cardinali, F. Hjort, N. Prokop, *et al.*, *Appl. Phys. Lett.* **121**, 103501 (2022).
24. Y. Mei, T. R. Yang, W. Ou, *et al.*, *Fund. Res.* **1**, 684 (2021).
25. Z. M. Zheng, Y. Mei, H. Long, *et al.*, *IEEE Electron Device Lett.* **42**, 375 (2021).
26. Y. F. Cheung, K. H. Li, and H. W. Choi, *ACS Appl. Mater. Interfaces* **8**, 21440 (2016).